



# Effect of Wind Direction on Airflow and Pollutant Dispersion Inside a Street Intersection

Huang Lihua, Huang Yuandong<sup>†</sup>, He Wenrong, Huang Liming and Ren Yixin

School of Environment and Architecture, University of Shanghai for Science and Technology, Shanghai, 200093, China

<sup>†</sup>Corresponding Author: Huang Yuandong

Nat. Env. & Poll. Tech.  
Website: [www.neptjournal.com](http://www.neptjournal.com)

Received: 18-5-2014

Accepted: 6-7-2014

## Key Words:

Airflow  
Pollutant dispersion  
Wind direction  
Street intersection  
Computational fluid dynamics

## ABSTRACT

The airflow and pollutant dispersion inside a street intersection under six different wind directions ( $\theta=0^\circ$ ,  $\pm 10^\circ$ ,  $\pm 30^\circ$  and  $45^\circ$ ) were evaluated using the computational fluid dynamics (CFD) approach. The numerical results reveal that the flow and pollutant dispersion inside a street intersection are greatly influenced by the incoming wind direction: (1) The air exchange between the outer flow and the intersection interior is the strongest under the wind direction angles of  $\pm 10^\circ$ , while it is the weakest for the wind direction angle of  $45^\circ$ ; (2) the pollutants from the intersection centre at the ground level are transported into the different streets depending on the various wind directions.

## INTRODUCTION

Vehicular exhaust emissions have become one of the major sources of air pollution in cities. Since, the pollutants from vehicle emissions (such as the carbon monoxide, hydrocarbons, nitrogen oxides, particulates) are detrimental to people's health, the dispersion of vehicle exhaust in streets canyons has become a focal point in environmental research (Huang et al. 2009).

Wind tunnel experiments (Gromke & Ruck 2007, Kastner-Klein et al. 2001, Kastner-Klein & Fedorovich 2002) and CFD simulations (Assimakopoulos et al. 2003, Takano & Moonen 2013, Huang et al. 2014) have been adopted widely to investigate flow and pollutant dispersion inside street canyons. A street intersection is often composed of four street canyons, where high pollution levels are frequently observed. The study of flow and dispersion in street intersections has been focused on the impact of geometry of intersection on flow field and pollutant distribution (Soulhac et al. 2009, Wang & McNmarab 2007). Up to now, however, the effect of wind direction on flow and pollutant dispersion in street intersections has not been studied intensively.

The objective of this study is to reveal the impact of wind direction on flow and dispersion inside a street intersection. In order to do so, we have chosen the six different wind directions. And the flow field and pollutant concen-

tration contours under each of the six wind directions were evaluated using the CFD approach.

## PHYSICAL MODEL

The three-dimensional physical model was employed in the CFD simulation as shown in Fig. 1. The four identical rectangular buildings were placed symmetrically to form a street intersection. Each rectangular building is 0.25 m long, 0.25m wide and 0.12m high. The width of each street is 0.06m. A pollutant point source at the ground level is situated at the centre of the intersection.

The computational domain is 2.36m long, 1.76m wide and 2m high. In order to examine the influence of wind direction on flow and pollutant dispersion inside a street intersection, six different incoming wind directions were considered in the present study. The angles (Fig. 2) of the incoming wind directions were  $\theta=0^\circ$ ,  $\pm 10^\circ$ ,  $\pm 30^\circ$  and  $45^\circ$ , respectively.

## CFD MODEL

**Governing equations:** The airflow inside a street intersection can be regarded as an incompressible flow. The governing equations for airflow are the Reynolds Averaged Navier-Stokes equations coupled with the Realizable k- $\epsilon$  turbulence model. And the governing equation for pollutant dispersion is the convection-diffusion equation for passive species transport, which is expressed as:

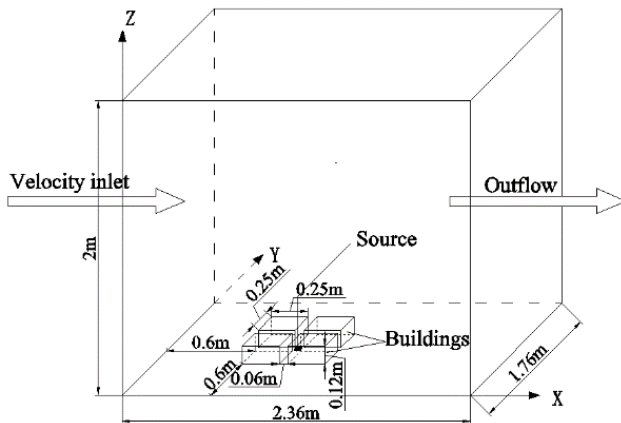


Fig. 1: The configuration of the street intersection and the computational domain.

$$U_j \frac{\partial C^\alpha}{\partial x_j} = \frac{\partial}{\partial x_j} \left( \left( D^\alpha + \frac{v_t}{Sc_t} \right) \frac{\partial C^\alpha}{\partial x_j} \right) \quad \dots(1)$$

Where  $U_j$  is the  $j^{\text{th}}$  mean velocity component;  $x_j$  is the Cartesian coordinate;  $C^\alpha$  is the concentration of pollutant species  $\alpha$ ;  $D^\alpha$  is the molecular diffusivity of species;  $v_t$  is the turbulent viscosity; and  $Sc_t$  is the turbulent Schmidt number.

**Boundary conditions:** At the inlet plane, the profile of horizontal wind velocity is specified as follows:

$$U_z = U_{ref} \left( \frac{z}{H_{ref}} \right)^\alpha \quad \dots(2)$$

Where,  $U_{ref} = 5.0\text{m/s}$ ,  $H_{ref} = 0.4\text{m}$ ,  $z$  is the height above the ground floor and  $\alpha = 0.22$ .

The outflow condition is adopted at the outlet plane. The non-slip condition is imposed at the ground and the building surfaces. A symmetry condition is utilized at the top of the domain and at the two side planes.

A mixture of ethane (pollutant) and air are released continuously from the point source. And the discharge rate for ethane is set to be  $0.03005 \text{ kg}/(\text{m}^3 \cdot \text{s})$ .

**Mesh generation:** The uniform grids are used inside the intersection. The grid cell is  $4 \times 10^{-3} \text{ m}$  in side, which is a mixed tetrahedral and hexahedral unstructured grid. The non-uniform grids are used in the other computational domain. The initial grid cell is  $4 \times 10^{-3} \text{ m}$  in side and the maximum size is  $50 \times 10^{-3} \text{ m}$  with an expansion ratio of 1.2. The total number of the grid cells in the domain is about 350000.

Due to the small point pollutant source, the grid cell for pollutant source is  $0.5 \times 10^{-3} \text{ m}$  in side.

**Numerical method:** All the simulations are conducted with

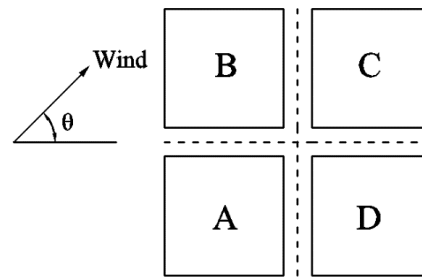


Fig. 2: Structure of the street intersection under the incoming wind direction angle  $\theta$ .

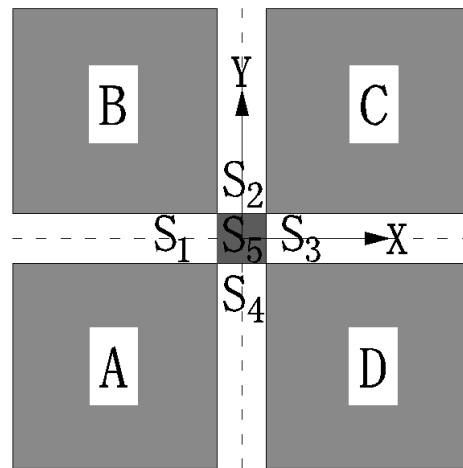


Fig. 3: Positions of the five sections.

Table 1: Air flux on the plane  $S_3$  under different incoming wind directions.

Wind direction angle	Air flux ( $\text{m}^3/\text{s}$ )
$-30^\circ$	0.00253
$-10^\circ$	0.00280
$0^\circ$	0.00185
$10^\circ$	0.00279
$30^\circ$	0.00257
$45^\circ$	0.00123

Table 2: Percentage of air flux through each section to the air flux through section  $S_1$  under various wind directions (negative value represents that the mean velocity on this section is deviated from the centre of the intersection).

$\theta$	$Q_1$ (%) ( $x < 0$ )	$Q_2$ (%) ( $y > 0$ )	$Q_3$ (%) ( $x > 0$ )	$Q_4$ (%) ( $y < 0$ )	$Q_5$ (%) ( $z > 0$ )
$0^\circ$	100.0	-0.8	-86.4	-0.6	-12.8
$10^\circ$	100.0	46.5	-62.6	-54.7	-24.9
$30^\circ$	100.0	127.1	-79.9	-111.7	-29.9
$45^\circ$	100.0	103.9	-90.6	-102.7	-14.5
$-10^\circ$	100.0	-57.6	-64.2	43.8	-24.2
$-30^\circ$	100.0	-110.8	-85.4	126.4	-30.2

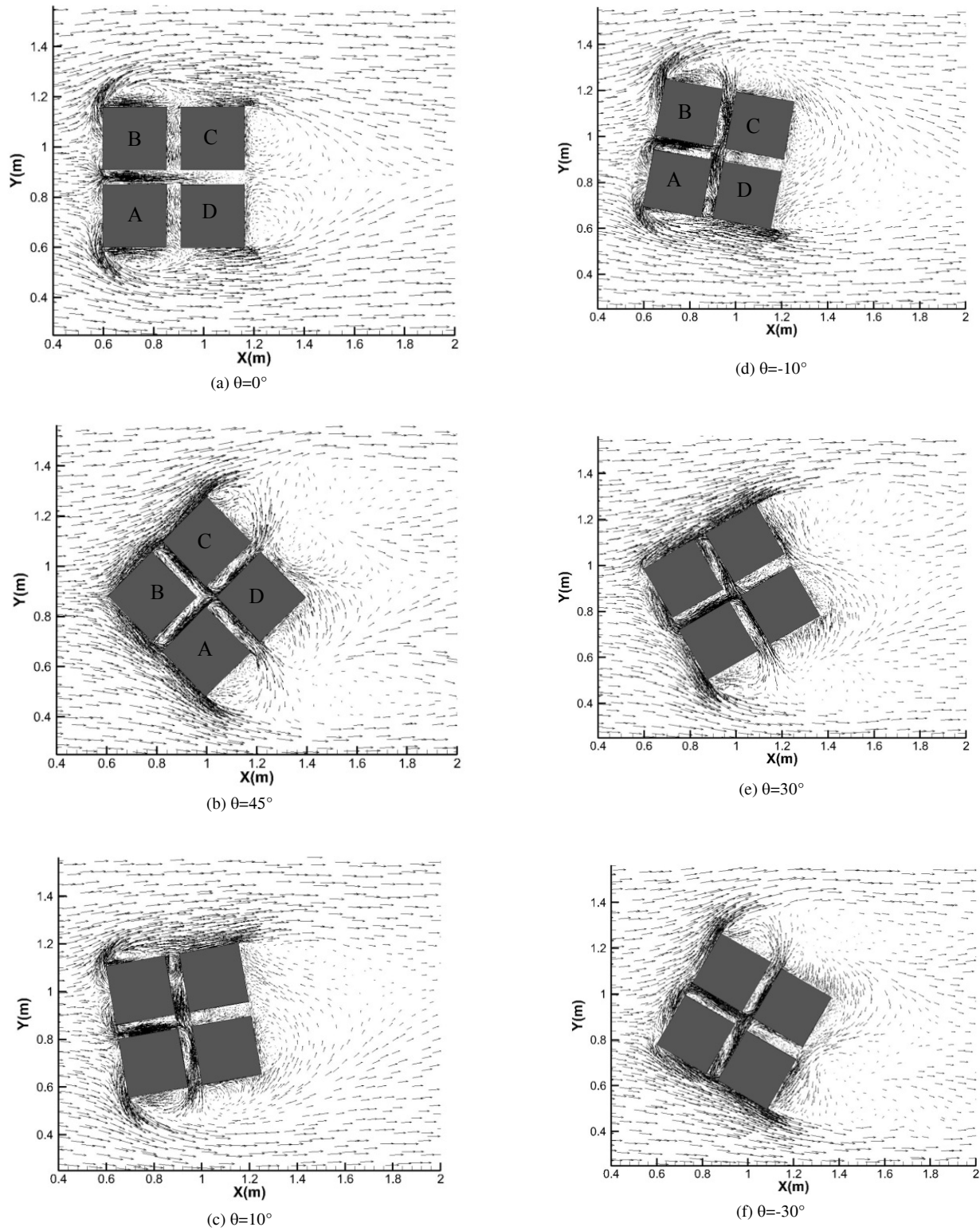


Fig. 4: Distribution of velocity vectors on the plane with  $z = 0.012$  m for different wind directions.

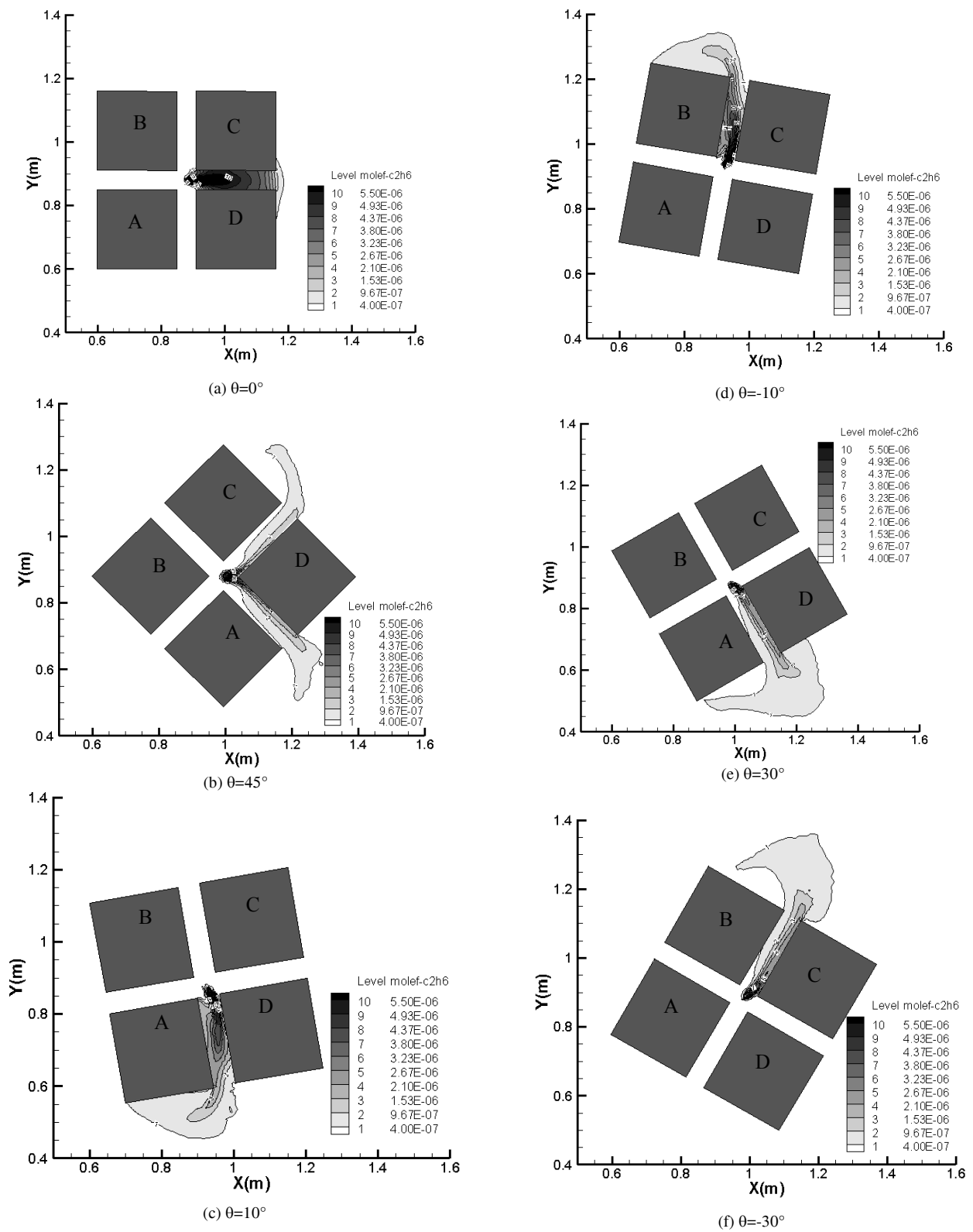


Fig. 5: Pollutant concentration contours on the plane with  $z = 0.012\text{m}$  for different wind directions.

the FLUENT code. The SIMPLE algorithm is used to handle the pressure-velocity coupling. The second order upwind-scheme is used for the discretization of equations for momentum, turbulent kinetic energy, turbulence dissipation rate and pollutant dispersion.

## NUMERICAL RESULTS AND DISCUSSION

**Air flux:** In order to analyse the air exchange between the intersecting streets and the air exchange between the outer flow ( $z > 0.12$  m) and the intersection interior ( $z \leq 0.12$  m), we have chosen the five cross-sections around the intersection centre as shown in Fig. 3. Here, a closed space is formed by the five sections and the ground. The height and width of each vertical section ( $S_1, S_2, S_3$  and  $S_4$ ) are 0.12 m and 0.06 m, respectively. Both, the length and width of the horizontal section  $S_5$  ( $z = 0.12$  m) is 0.06 m.

The air flux on the section  $S_5$  is crucial for the reduction of pollution level inside the intersection. Based on the calculated velocity fields, the air flux through the section  $S_5$  is obtained under the six different incoming wind directions (Table 1). From this table, it is evident that the wind direction has a great influence on the air exchange between the outer flow and the intersection interior. Among the six incoming wind directions, the air flux through the plane  $S_5$  is the largest for the angle of  $\pm 10^\circ$ , and is the smallest under the wind incoming angle of  $45^\circ$ .

**Air flux through each section:** The air flux through each section can be obtained from the computed flow fields. The percentage of air flux through each section to the air flux through the section  $S_1$  is given in Table 2. From this Table, it is seen that the  $Q_3$  and  $Q_5$  are negative under all the six studied wind directions, suggesting that air flows out of the intersection through the sections  $S_3$  and  $S_5$ , while, the airflow directions through the sections  $S_2$  and  $S_4$  depends on the incoming wind directions. From Table 2, it can also be observed that the air flux through each section is greatly influenced by the inflow wind direction. And the larger the absolute value of wind direction angle is, the greater the air flux through each section is (when the absolute value of the wind direction angle is in the range of  $10^\circ$  to  $30^\circ$ ).

**Airflow field:** Fig. 4 shows the distribution of velocity vectors on the plane with  $z = 0.012$  m for six different wind directions. From this figure, it is obvious that the flow in the streets is related to the incoming wind direction. For example, the air flows from the centre of the intersection towards the street formed by the buildings C and D for  $\theta = 0^\circ$ . For the cases with  $\theta = -10^\circ$  and  $-30^\circ$ , the air at the centre of the intersection flows into the street formed by the buildings B and C, while the air flows into the street formed by the buildings A and D for the cases with  $\theta = 10^\circ$  and  $30^\circ$ . Especially

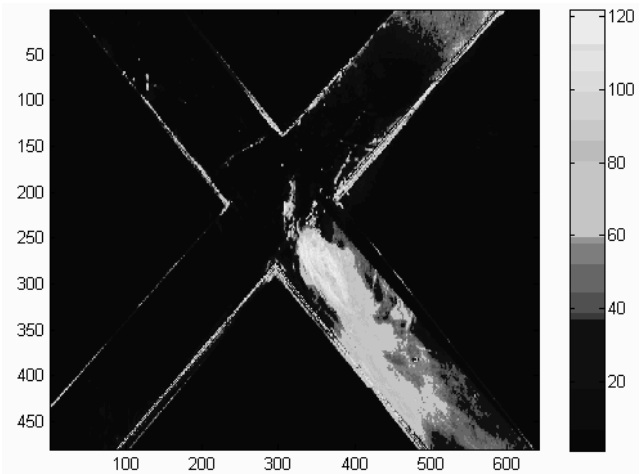


Fig. 6: Pollutant distribution obtained in the wind tunnel experiment for the intersection under the incoming wind direction angle of  $30^\circ$ .

for the case with  $\theta = 45^\circ$ , the air at the intersection centre flows partly into the street formed by the buildings C and D and partly into the street formed by the buildings A and D.

**Pollutant dispersion:** Fig. 5 shows the pollutant concentration contours on the plane with  $z = 0.012$  m for six different wind directions. From this figure, it is apparent that the pollutant dispersion inside the street intersection is also influenced greatly by the incoming wind direction. The pollutant dispersion is decided by the airflow field, and thus the pollutants from the point source are transported into the street formed by the buildings C and D for  $\theta = 0^\circ$ , into the street formed by the buildings B and C for the cases with  $\theta = -10^\circ$  and  $-30^\circ$ , and into the street formed by the buildings A and D for the cases with  $\theta = 10^\circ$  and  $30^\circ$ . Especially for the case with  $\theta = 45^\circ$ , the pollutants from the point source are conveyed partly into the street formed by the buildings C and D and partly into the street formed by the buildings A and D.

## COMPARISON OF NUMERICAL RESULTS WITH WIND TUNNEL EXPERIMENT

We have conducted a wind tunnel experiment to investigate the pollutant dispersion in the street intersection for the incoming wind direction with  $\theta = 30^\circ$ . In the physical modelling, the configurations of the street intersection and the point source are the same as those shown in Fig. 1. The free stream velocity is 5 m/s in the wind tunnel experiment. Fig. 6 shows the pollutant distribution obtained in the wind tunnel experiment. By comparing Fig. 5(e) with Fig. 6, it is observed that the pollutant dispersion pattern obtained from the CFD simulation is very similar to that obtained from the wind tunnel experiment.

## CONCLUSION

The airflow and pollutant dispersion inside a street intersection under six different wind directions ( $\theta = 0^\circ, \pm 10^\circ, \pm 30^\circ$  and  $45^\circ$ , respectively) are simulated using the CFD approach. The numerical results reveal clearly that the flow field and pollutant distribution inside a street intersection are greatly influenced by the incoming wind direction:

1. The air exchange between the outer flow and the intersection interior is the strongest under the wind direction angles of  $\pm 10^\circ$ , while it is the weakest for the wind direction angle of  $45^\circ$ .
2. At the intersection centre, the pollutants from the point source situated at the ground level are transported into the different streets depending on the various wind directions.

## ACKNOWLEDGEMENT

This study was supported by the Innovation Fund Project for undergraduate students of Shanghai (SH1110252095).

## REFERENCES

- Assimakopoulos, V. D., ApSimon, H. M. and Moussiopoulos, N. 2003. A numerical study of atmospheric pollutant dispersion in different two-dimensional street canyon configurations. *Atmospheric Environment*, 37: 4037-4049.
- Gromke, C. and Ruck, B. 2007. Influence of trees on the dispersion of pollutants in an urban street canyon - experimental investigation of the flow and concentration field. *Atmospheric Environment*, 41: 3287-3302.
- Huang, Y.D., Hu, X.N. and Zeng, N.B. 2009. Impact of wedge-shaped roofs on airflow and pollutant dispersion inside urban street canyons. *Building and Environment*, 44: 2335-2347.
- Huang, Y.D., Long, C., Deng, J.T. and Kim, C.N. 2014. Impacts of upstream building width and upwind building arrangements on airflow and pollutant dispersion in a street canyon. *Environmental Forensics*, 15: 1-12.
- Kastner-Klein, P. and Fedorovich, E. 2002. Diffusion from a line source deployed in a homogeneous roughness layer: interpretation of wind tunnel measurements by means of simple mathematical models. *Atmospheric Environment*, 36: 3709-3718.
- Kastner-Klein, P., Fedorovich, E. and Rotach, M.W. 2001. A wind tunnel study of organized and turbulent air motions in urban street canyons. *Journal of Wind Engineering and Industrial Aerodynamics*, 89(9): 849-861.
- Soulhac, L., Garbero, V., Salizzoni, P., Mejean, P. and Perkins, R.J. 2009. Flow and dispersion in street intersections. *Atmospheric Environment*, 43(18): 2981-2996.
- Takano, Y. and Moonen, P. 2013. On the influence of roof shape on flow and dispersion in an urban street canyon. *Journal of Wind Engineering and Industrial Aerodynamics*, 123: 107-120.
- Wang, X. and McNmarab, K.F. 2007. Effects of street orientation on dispersion at or near urban street intersections. *Journal of Wind Engineering and Industrial Aerodynamics*, 95: 1526-1540.